Power-Limited Contraction Dynamics of *Vorticella convallaria*: An Ultrafast Biological Spring

A. Upadhyaya,* M. Baraban,* J. Wong,* P. Matsudaira,† A. van Oudenaarden,* and L. Mahadevan‡
*Department of Physics and G. R. Harrison Spectroscopy Laboratory, †Whitehead Institute for Biomedical Research, Biological Engineering Division, and Department of Biology, Massachusetts Institute of Technology, Cambridge, Massachusetts; and ‡School of Engineering and Applied Sciences and Department of Organismic and Evolutionary Biology, Harvard University, Cambridge, Massachusetts

ABSTRACT *Vorticella convallaria* is one of the fastest and most powerful cellular machines. The cell body is attached to a substrate by a slender stalk containing a polymeric structure—the spasmoneme. Helical coiling of the stalk results from rapid contraction of the spasmoneme, an event mediated by calcium binding to a negatively charged polymeric backbone. We use high speed imaging to measure the contraction velocity as a function of the viscosity of the external environment and find that the maximum velocity scales inversely with the square root of the viscosity. This can be explained if the rate of contraction is ultimately limited by the power delivered by the actively contracting spasmoneme. Microscopically, this scenario would arise if the mechanochemical wave that propagates along the spasmoneme is faster than the rate at which the cell body can respond due to its large hydrodynamic resistance. We corroborate this by using beads as markers on the stalk and find that the contraction starts at the cell body and proceeds down the stalk at a speed that exceeds the velocity of the cell body.

INTRODUCTION

Nature utilizes a diverse range of designs to generate movement at cellular and molecular levels. Of these, one of the fastest is found in stalked protozoans such as *Vorticella*. *Vorticella* is composed of a cell body (known as the zooid, 30–40 μm in diameter) and a long, slender stalk (100–200 μm in length and 2–3 μm in diameter) that is tethered to a substrate by a natural adhesive that is secreted by the cell. Living *Vorticella* contract extremely rapidly, either spontaneously or if stimulated mechanically (1), traversing ~5000 times their length per second. The organelle responsible for contraction is the spasmoneme, which is placed helically within the stalk's outer elastic sheath (2,3) as shown in Fig. 1. A major spasmoneme protein, spasmin, has been implicated as a calcium-binding protein that drives the contraction (4,5). In live cells, contractions are preceded by a rise in the calcium level in the cell body (6). The calcium signal is then thought to propagate down the stalk by calcium released from membrane stores within the spasmoneme, triggering the contraction (2,4), consistent with experiments on *Vorticella* stalks treated in glycerol to permeabilize the membrane. The stalks of glycerinated *Vorticella* contracts on the addition of Ca^{2+} and reextends when Ca^{2+} is removed using a calcium chelating agent such as EDTA or EGTA (2,7–9).

The contraction is reversible and can be repeated many times without the addition of ATP (10). This contractile motility is fundamentally different from many other types of cell motility, for example those powered by ATP, such as myosin sliding along actin filaments or actin and microtubule polymerization (10). Shrinkage and swelling of the spasmoneme in the presence or absence of calcium (11) suggests that active elasticity of *Vorticella* resembles that of a polyelectrolyte gel (12). In the absence of calcium, spasmin filaments are thought to be a bundle of negatively charged, roughly parallel filaments that are weakly cross-linked (2,3,13,14) (Fig. 1). In the extended state, the tendency of a weakly cross-linked polymer network to collapse entropically is resisted by the electrostatic repulsion forces between the negatively charged filaments. Calcium binding neutralizes the charges and leads to an entropic collapse of the spasmoneme, which then powers the helical coiling of the stalk. After contraction, the stalk uncoils and reextends spontaneously, presumably due to the electrostatic repulsion associated with the unbinding of calcium from the spasmoneme and elastic recoil of the stalk sheath.

The timescale of contraction of glycerinated *Vorticella* is more than two orders of magnitude slower than the contraction of live cells. To uncover the contractile mechanism, it is therefore important to perform quantitative experiments on live cells. A few studies have investigated the contraction of live cells with high speed imaging (15,16). Moriyama et al. (16) described the spasmoneme as a simple damped spring. However, the damped spring model is not sufficient to describe the entire contraction, as it does not account for the initial stages of motion when the active processes that cause the spasmoneme to contract are at play. Furthermore, prior studies have not quantified the effects of the external load on the dynamics of contraction. To remedy this, we use high speed microscopy to measure the contraction velocity and effective force of contraction as a function of increasing viscous load. We find that we must account for an actively contracting spring to describe our results for the dynamics of contraction. A consideration of

Submitted March 13, 2007, and accepted for publication July 30, 2007.

Address reprint requests to Arpita Upadhyaya, E-mail: arpitau@umd.edu; or L. Mahadevan, E-mail: lm@seas.harvard.edu.

Editor: Alexander Mogilner.

0006-3495/08/01/265/08 $2.00

doi: 10.1529/biophysj.107.108852

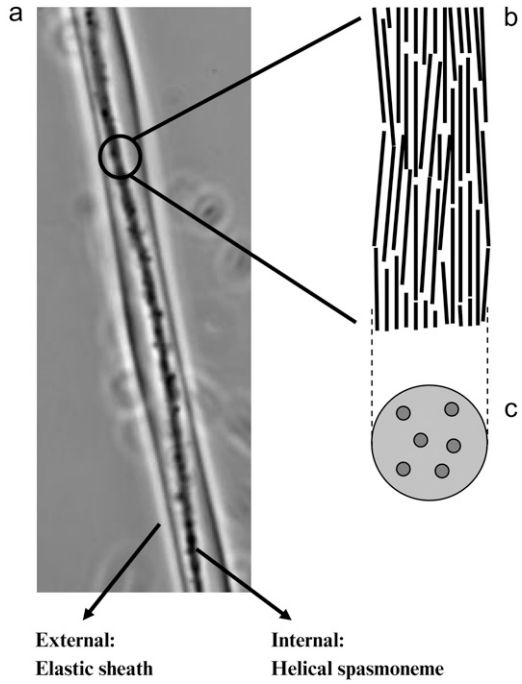

FIGURE 1 Internal structure of the *Vorticella* spasmoneme. (*a*) A phase contrast image of a portion of the *Vorticella* stalk. A helically coiled spasmoneme can be seen inside an external elastic sheath. The length shown corresponds to 80 μm. (*b*) A schematic diagram of the internal structure of the spasmoneme showing roughly aligned bundles of spasmin filaments. (*c*) A schematic cross section of the spasmoneme showing the presence of putative membrane bound calcium stores.

the external hydrodynamics induced by the movement of the organism, along with the observed burst of calcium in the zooid (6), and our measurements of the contraction velocity at different points along the stalk strongly constrain the mechanism of calcium propagation and the dynamics of contraction and lead to a simple picture for the process.

MATERIALS AND METHODS

Cell culture and imaging

Vorticella convallaria cells were obtained from the Buhse laboratory (University of Illinois, Chicago). The culture methods were adapted from Vacchiano et al. (17). The culture medium was prepared by mixing 2 g of wheat grass powder (Pines International, Lawrence, KS) with water, boiling for a few minutes, then filtering and autoclaving. This was diluted in half with spring water before use for cell culture. Cells were grown in a culture medium with bacteria in 500 ml flasks at room temperature. To harvest cells for experiments, the culture flasks were shaken overnight to detach cells from the flask surface. *Vorticella* cells were separated from the media, bacteria, and other debris using a set of 35 μm and 6 μm filters. The filtered cells were seeded into petri dishes in an inorganic medium (IM; 0.24 mM $MgS0_4$ and 0.24 mM NaCl). Thin strips of glass were placed in the dishes to serve as substrate for cell attachment. Samples were prepared about 3 days before an experiment to allow time for cells to spontaneously attach and grow.

Cells attached to vertical sides of the glass strips were used for imaging, as the stalks were parallel to the horizontal plane. For our experiments we imaged spontaneous cell contractions, which occurred every few minutes. Cells were imaged using an inverted microscope (Nikon Eclipse TE300, Nikon Instruments, Melville, NY) connected to a high speed camera (Kodak Ektapro HS Motion Analyzer, Model 4540mx Imager, Eastman Kodak, Rochester, NY) at 9000 or 13,500 frames per second using 20× or 40× objective lenses. In the resulting digital images using a 40× objective lens, 1 pixel corresponded to 1 micron. For the cell coordinate tracks, $t = 0$ was defined as the time at which the cell body started moving. The images were analyzed by tracking either the cell body or beads attached to different parts of the stalk and zooid to obtain the *x-y* coordinates using Metamorph software (Universal Imaging, West Chester, PA). These data were then further analyzed using MATLAB (Mathworks, Natick, MA). The measurement error for length measurement was less than 1 pixel.

Viscosity modification and bead attachment

Polyvinyl pyrrolidone (PVP-K90 from Sigma-Aldrich, St. Louis, MO) of molecular weight 360,000 was used as a viscosity modifying agent. PVP was dissolved into inorganic media at concentrations ranging from 0.4% to 6% (w/v) to provide a viscosity range from 1 cP to ~45 cP. Different concentrations of PVP were prepared from the same stock solution at 6%. The viscosity was measured using a cone and plate viscometer. From these measurements we verified that the PVP solution at the concentrations used had negligible elastic modulus at the shear rates achieved. Before each experiment PVP solutions were mixed well and poured into petri dishes. To change the viscous environment of the cells, the glass strip with the selected cell was transferred from one dish to another with media of different viscosity, with an intermediate washing step. The attachment between the stalk and substrate was strong enough that the cells did not detach during the transfer process. The same contraction speeds were recovered if the cell was replaced in the original medium, which suggests that PVP did not affect the cell in an irreversible manner. For the bead experiments, polystyrene beads (Polysciences, Warrington, PA) of 2 μm diameter (1 μl of a 0.2% suspension) were mixed with 0.25 mg/ml poly-L-lysine and incubated at 4°C overnight. Beads were washed in IM and pipetted in small quantities around the cells. After a few minutes some cells had beads attached to them. Usually the attachment was strong and withstood many contractions.

RESULTS

Dynamics of *Vorticella* contraction

We observed the spontaneous contractions of living *Vorticella* cells using a high speed camera (9000 fps). Fig. 2 *a* shows time lapse images of a contraction. It takes ~6 ms for a stalk of length 150 μm to contract. The initially straight stalk bends and coils into a helix, starting from the region near the zooid and moving down toward the base of the stalk. During the contraction, the zooid moves without any observable rotation until the end of the contraction, in contrast to the observations of Moriyama et al. (16). After the stalk becomes fully coiled, the zooid starts rotating in a clockwise direction (movie in Supplementary Material). Subsequently the stalk reextends and returns to its original length. The reextension takes a few seconds.

Based on the exponential decay of stalk length and velocity, previous studies have modeled the *Vorticella* stalk contraction as a damped spring (16) in which the contractile force exerted by the *Vorticella* is balanced by the viscous drag on the cell body. This description is valid only during the passive phase of the movement, during which the fluid

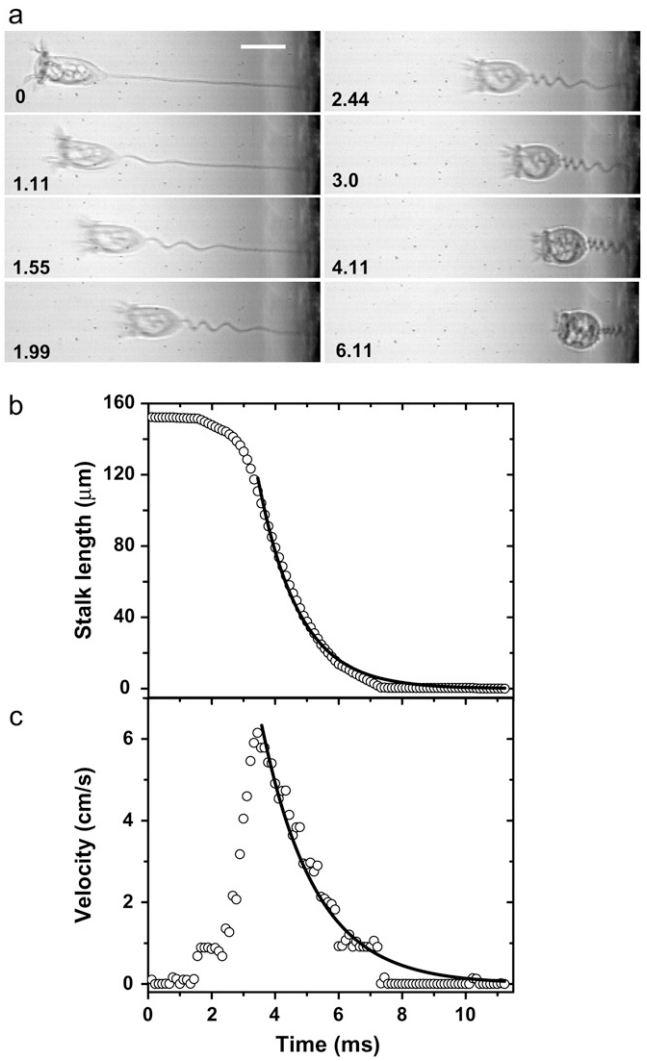

FIGURE 2 Dynamics of *Vorticella* contraction. (*a*) Time series of contraction (time shown in ms). The scale bar is 35 μm. (*b*) *Vorticella* stalk length as a function of time during a contraction. The solid curve is an exponential fit. (*c*) Instantaneous velocity of the cell body as a function of time. The solid curve is an exponential fit to the decaying part of the velocity.

forces on the cell body slow down the stalk after the contractile forces are fully activated, i.e., once the calcium is completely bound everywhere along the spasmoneme. On the other hand, during the early stages of contraction, this simple spring picture clearly cannot be complete due to the effect of fluid inertial effects as well as the dynamics of the active contractile processes associated with calcium dynamics, binding, and spasmoneme contraction. We therefore studied the kinetics of contractility at short times by separately tracking the contraction of the stalk as well as the movement of the cell body through the external fluid environment and used the data obtained therein to determine the forces associated with contraction.

The coordinates of the junction between the stalk and zooid were tracked to determine the position of the cell body and stalk length, the distance between the cell body and the point of attachment of the stalk to the substrate, as a function of time. The length of the stalk as a function of time is plotted in Fig. 2 *b*, with the fully contracted stalk length assumed to be zero (a reasonable approximation given how small it is relative to its extended form). The instantaneous velocity was obtained from the distance traveled during the time interval between frames and is plotted in Fig. 2 *c*. The position and velocity data of different cells showed the same qualitative behavior, i.e., a rapid increase in the velocity for $\sim$2 ms until it attains a maximum, after which it decays exponentially to zero. The maximum velocity obtained varied from cell to cell but was relatively constant between different contractions for the same cell.

Effect of external viscosity on contraction dynamics

We first studied the effect of the external viscosity of the medium on the dynamics of contraction. Fig. 3 *a* shows the

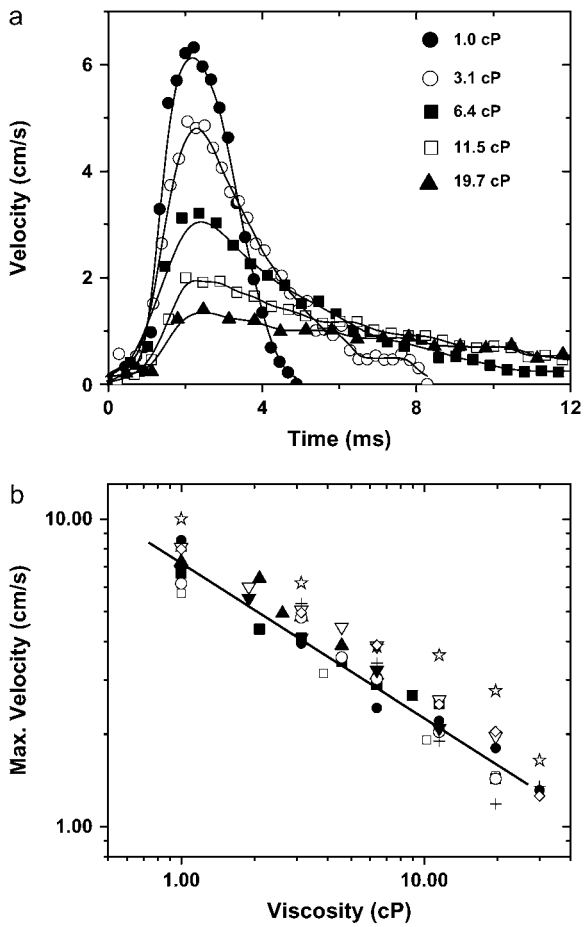

FIGURE 3 Viscosity dependence of *Vorticella* contraction velocity. (*a*) Plot of the instantaneous cell velocity as a function of time for different viscosities for a single cell. (*b*) Double logarithmic plot of the maximum contraction velocity as a function of the viscosity for several cells. The solid line has a slope of -0.5.

velocity profiles for a single cell in media with different external viscosities. As expected, the maximum velocity decreases as the viscosity increases and the time taken to complete a contraction increases. The time taken to reach the maximum velocity is independent of the viscosity and takes ~2.5 ms. A plot of the maximum velocity as a function of viscosity for several different cells (Fig. 3 *b*) shows the same trend for all cells and can be described by a power law behavior with $u \approx \eta^{-0.50\pm0.03}$. The data represent contractions recorded from 10 different cells plotted simultaneously. Each data point is an average of three or four contractions of a cell at a particular viscosity.

Previous studies of *Vorticella* contraction have modeled it as a damped spring (16). This is clearly only relevant during the passive decaying phase of the movement, when the contractile force production mechanism is no longer active. The simplest picture of this passive process leads to a model for the stalk behaving like a spring that pulls the cell body through a viscous fluid. Then, assuming that fluid inertia is not important, we may write $kx = -6\pi\eta r(dx/dt) = 6\pi\eta r u$, where k is the spring constant, η is the viscosity of the medium, u is the velocity, and r is the radius of the cell body. This leads to exponentially decaying solutions for the stalk length (x) and the velocity (u) as a function of time. From our experimental data, we do observe an exponential decay of the velocity as well as stalk length for the regime of motion after the initial rise in velocity, as shown by the fits in Fig. 2, *b* and *c* (*solid lines*) and $x(t) = L_o \exp(-kt/6\pi\eta r)$ with a time constant.

The position decays as $x(t) = L_o \exp(-kt/6\pi\eta r)$ with a time constant $\tau = 6\pi\eta r/k$. Thus, $k = -6\pi\eta r/\tau$ is a measure of the effective spring constant. We find that $k = 0.33 \pm 0.06$ dyn/cm averaged over 10 cells in water (similar to the results of Moriyama et al. (16)). However, if a simple spring model holds and the viscous drag forces are the dominant forces opposing contraction, then the maximum velocity should scale as η^{-1}. This is clearly not so and thus our experimental results require a different explanation. Instead our experiments are consistent with earlier biochemical and kinetic measurements (2,7,14) that the spasmoneme is an active mechanochemical spring that contracts ever more strongly as the calcium binds to it, so that the force increases dynamically even as the stalk contracts to relax the strain in the spasmoneme.

This picture leads naturally to a deceptively simple explanation of the power law dependence of the maximum velocity on the viscosity. Since the viscous power dissipated by the movement of a spherical cell body moving in the low Reynolds regime is given by $P \approx \eta r u^2$, it immediately follows that in a power-limited situation, $u \approx \eta^{-1/2}$. As we shall see, this is consistent with the situation here wherein a wave of calcium binding triggers a wave of entropically driven polymer collapse that provides the driving power for the contraction; since this is ultimately limited, we expect that the maximum velocity of contraction must follow the above scaling law. Fig. 4 *a* shows that the power dissipated

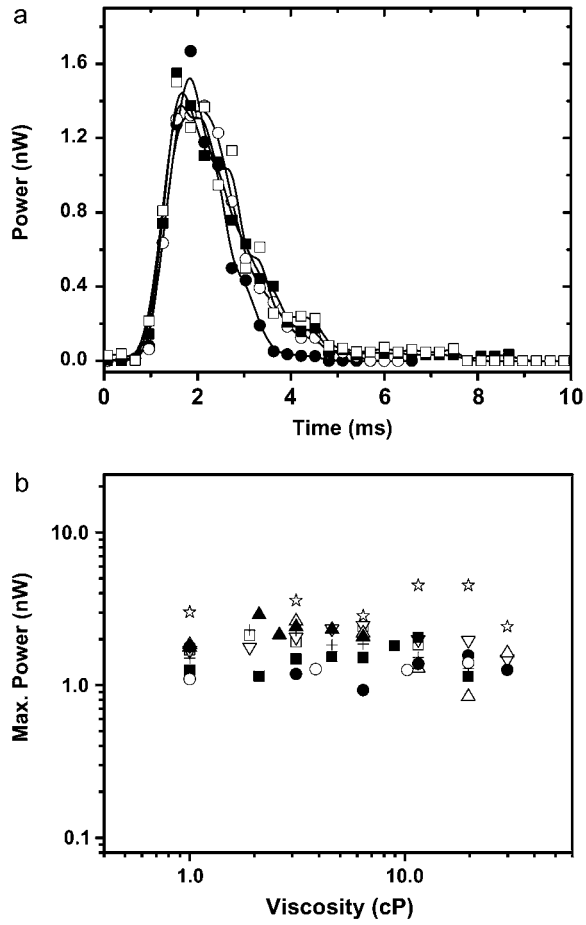

FIGURE 4 Instantaneous power dissipated during a contraction as a function of time. (*a*) The hydrodynamic dissipation rate as a function of time shows that the data for different viscosities collapses onto a single master curve. Symbols correspond to the legend for Fig. 3. (*b*) The maximum power as a function of the viscosity is constant as expected based on theoretical arguments.

calculated using the Stokes drag on the cell body during contraction, i.e., $P = 6\pi\eta r u^2$ is indeed independent of the ambient viscosity. In Fig. 4 *b* we see that the maximum power dissipated is thus independent of the viscosity and is of the order of a nW.

Time-resolved dynamics of the stalk during contraction

Since stalk contraction is powered by calcium release, an important question is the role of extrinsic versus intrinsic dynamics in determining the rate of contraction. In one extreme limit, if the viscosity of the external fluid was low (or equivalently the cell body was absent) the resistance to contraction would be vastly reduced, so that one might expect that the observed rate of contraction is determined primarily by the rate of calcium binding and spasmoneme contraction. In the other limit, if the external fluid were

highly viscous, the rate of contraction is limited by the (in)ability of the cell body to respond rapidly to spasmoneme contraction, so that the external environment is what dominates.

A further complication arises due to the spatially extended nature of the spasmoneme bundle and stalk. For simultaneous calcium release along the stalk, all points on the stalk should start moving simultaneously. On the other hand, if a wave of calcium release (and thence contraction) from the cell body propagates down the stalk activating the spasmoneme along its length, points closer to the cell body should start moving earlier than points closer to the base. To distinguish between these scenarios, we tracked the stalk at different points along its length. To visualize the stalk motion in greater detail, we decorated the *Vorticella* stalk at different points with poly-lysine-coated beads as markers. The bead movement was tracked using a particle-tracking algorithm. Fig. 5 *a* shows a time series of a contracting *Vorticella* with two beads along its stalk. From the images we can clearly see that there is a finite time delay between the motion of the cell body and that of the bead nearest to the base of the stalk. Fig. 5 *b* shows the instantaneous velocity plots of the cell body and the two beads. Motion is initiated first in the cell body and then in the bead closest to it and finally in the bead farthest from the body, indicating that the contraction begins at the body and travels down the stalk. This allows us to define a signal propagation velocity $v_{\text{wave}} = \Delta x/\Delta t$, where Δx is the distance between the cell body and that bead and Δt is the time interval between the movement of the cell body and first detectable movement of the bead nearer to the base.

To study the dependence of this signal propagation on the external environment, we repeated the experiments in media of increasing viscosities, using the protocols described before. Fig. 5 *c* shows that the front propagation speed is nearly independent of viscosity, $v_{\text{wave}} \approx \eta^{-0.1}$, whereas the maximum velocities of the cell body as well as the bead scales as $v_{\text{max}} \approx \eta^{-0.5}$. These observations of the wave characterized by bead movement is the signature of an internal mechanochemical signal which propagates from the cell body down to the base of the stalk and is not affected by the external viscous environment. These conclusions are validated by additional experiments in which we held the cell body of a *Vorticella* in a micropipette while the stalk was not attached to a substrate. Even though the stalk was free while the body was held fixed, the contraction and coiling started near the cell body and then propagated to the base of the stalk (data not shown). We note that these observations are consistent with the idea that the rate-limiting step for the reaction is the wave of contraction that travels along the stalk; however the speed of the cell body is determined by its large viscous resistance.

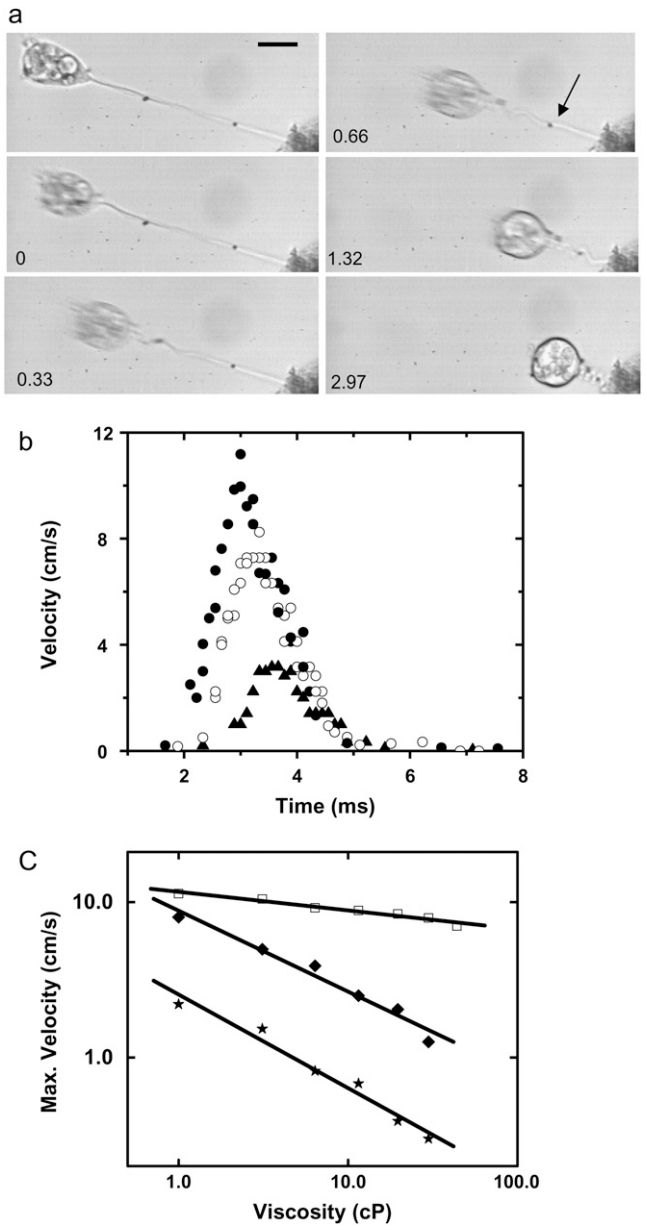

FIGURE 5 Spatially resolved stalk dynamics. (*a*) Time series of a contraction with two beads along the *Vorticella* stalk (time is in ms). The arrow indicates the frame when the second bead starts moving. The scale bar is 30 μm. (*b*) Time course of the instantaneous velocity of the cell body (*solid circles*), first bead (*open circles*), and second bead (*triangles*). (*c*) Effect of viscosity on the velocities plotted on a log-log scale: wave speed (*squares*), maximum velocity of cell body (*diamonds*), maximum velocity of bead (*stars*).

Calculation of forces during contraction

Although the observed scaling of the maximum velocity with $\eta^{-0.5}$ is consistent with a power-limited contractile spring, to calculate the force of contraction, we need to account for fluid inertia at short times during the acceleration phase of the cell body. Indeed, it is well known that this startup phase is quite different from the steady state that is assumed in applying Stokes law for the drag on a sphere due to the effects of fluid acceleration and viscous boundary layers. Accounting for these effects when the velocities are still

small enough so that we may neglect the nonlinearities inherent in the Navier-Stokes equations leads us to consider the solution of the unsteady Stokes equations (18). For a spherical particle (the cell body) moving with a velocity $u(t)$ under the influence of an external force $f(t)$ (due to the contracting stalk + spasmoneme), this yields an equation of motion (18),

$$2\pi r^3 \rho_f \dot{u} + 6\pi\eta r u + 6r^2\sqrt{\pi\eta\rho_f}\int_0^t \dot{u}\frac{d\tau}{\sqrt{t-\tau}} = f(t). \quad (1)$$

Here r is the radius of the cell body as before, η is the viscosity of the ambient fluid, ρ_f is the density of the ambient fluid (and also that of the cell body, which is mostly water). The prefactor in the inertial term arises from the added mass effect due to the fact that the fluid has to be moved by the cell body, the second term is the Stokes drag, and the third term arises due to the ''memory'' associated with the acceleration phase and is history dependent. Using the experimentally measured velocity $u(t)$ and neglecting any contributions to the force on the cell body due to the complex geometry of the coiling stalk as well as the presence of the attachment boundary, this expression allows us to estimate the time course of the active force directly by numerically integrating Eq. 1. We estimated the radius from the rounded shape of the cell body during the exponential phase of the decay. A given cell goes through the same sequence of shape changes, regardless of the viscosity; hence the same radius was used for drag force calculations. In Fig. 6 *a*, we plot the maximum of the total force as a function of viscosity for five different cells (as calculated from Eq. 1).

We find that the maximum force of contraction increases with viscosity as $F \approx \eta^{0.48\pm0.03}$, a direct consequence of the power limited contraction, which yields $F \approx (P\eta r)^{1/2}$. In Fig. 6, *b* and *c*, we plot the time series of all the force terms (inertia, history, Stokes drag, and total force) for one representative cell at 1 cP (lowest viscosity case) and 11.5 cP, respectively. We find that the history-dependent term contributes at most ~20% of the total force in the early stages of the contraction (before the maximum velocity is achieved) for low viscosity. However, this term become negligibly small throughout the contraction at higher viscosities. Thus we can rule out the role of fluid inertia in determining the dynamics of contraction and the simple scaling law for the maximum velocity of contraction.

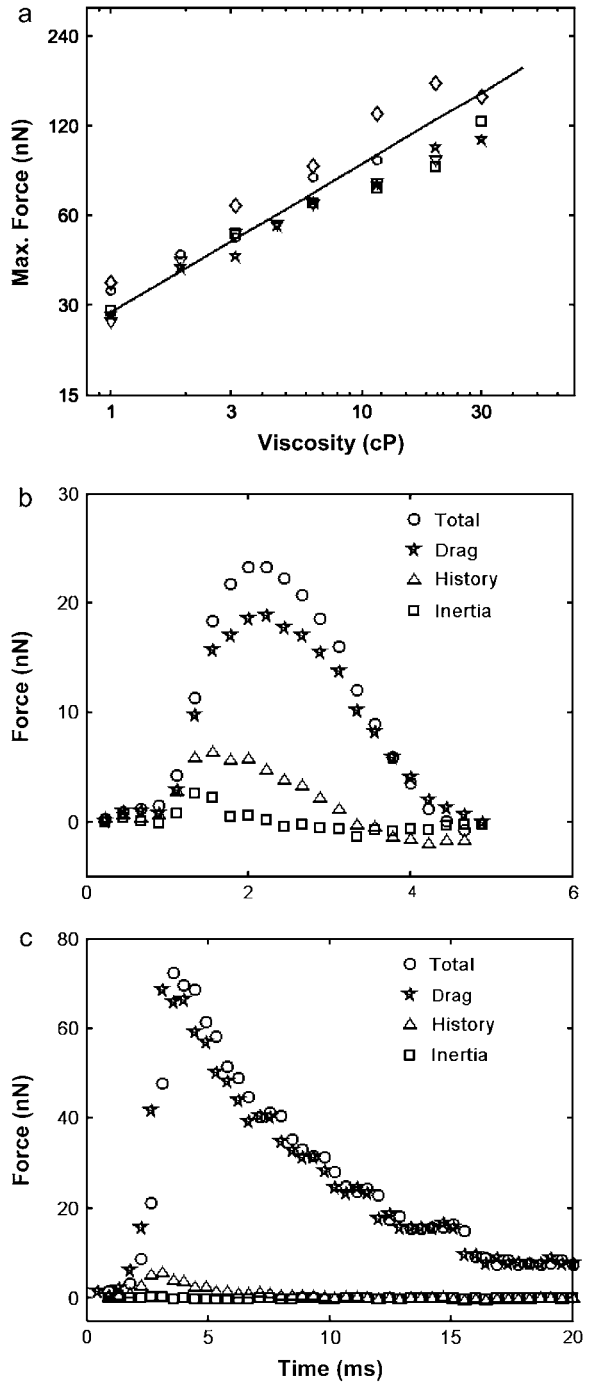

FIGURE 6 Effect of external viscosity on contraction force. (*a*) Double logarithmic plot of the maximum total force as a function of the viscosity for five cells, calculated from Eq. 1. The solid line has a slope of 0.5. (*b*) Time series of forces (inertia, history, drag, and total force) for a representative cell at 1 cP. These forces were calculated from Eq. 1. The total force is *f*, inertia is the term on the left, drag is the second term on the right, and history is the third term on the right. (*c*) Time series of forces for a representative cell at 11.5 cp. The forces are calculated as in *b*.

DISCUSSION

We have studied the dynamics of *Vorticella* contraction under different loading conditions by varying the viscosity of the medium. The initial rise in velocity and the dependence of the dynamics on viscosity are not consistent with a simple viscously damped spring model. Our observation that the stalk contracts faster than the cell body can respond is consistent with the fact that, in many cell biological systems,

calcium release occurs on the millisecond timescale, so that the force associated with polyelectrolyte collapse also arises on similar timescales. However, the cell body is unable to respond quickly enough due to the large resistance associated with accelerating and moving it through a viscous fluid. This allows the force to build up as more and more of the spasmoneme contracts in response to the wave of calcium that propagates along it. However, since the power provided by this binding is ultimately limited, the maximum velocity of contraction is determined by this fact. This explains the observed inverse square root dependence of the maximum velocity as a function of the viscosity.

Electron microscope observations show the presence of membrane tubules inside the spasmoneme that are putative calcium stores (2,4). Previous studies have proposed that the internal signal is a wave of calcium that propagates by calcium-induced calcium release. However, these diffusion-mediated are too slow (maximum speed of $\sim$100 μm/s (19)) to account for the observed speeds. Much higher speeds ($\sim$10 m/s) can be achieved by electrical signals (20). Some evidence for the existence of an electrical signal comes from the measurement of depolarization of the zooid membrane before contraction (21). The depolarization could evoke an action-potential-like signal that is transmitted along the membrane compartments inside the stalk using voltage-activated channels that induce the release of calcium. Subsequently, calcium can diffuse into the spasmoneme (diameter $\sim$1 μm), sequentially activating it along its length during the rising phase of the velocity (the first 2.5 ms). As sections of the spasmoneme get activated, the contractile force and velocity increase. Experimentally, we observe that the maximum velocity of contraction is reached at approximately the same time after triggering for different values of the environmental fluid viscosity. This implies that the cell body velocity rise is due to activation of the spasmoneme by the calcium wave—whose velocity of propagation is independent of the fluid viscosity (Fig. 5). The limits on the dynamics of contraction place a limit on the maximum power generated by the contracting spasmoneme; consequently, for a cell body moving in a viscous environment, the maximum velocity of contraction should be inversely proportional to the square root of the viscosity, as seen in our experiments.

Our results provide a framework in which *Vorticella* contraction may be modeled as an active mechanochemical spring (22). More broadly, it is worth pointing out that the basic protein involved in contraction, spasmin (4), is homologous to EF-hand domain proteins, e.g., centrins, which are ubiquitous components of microtubule-organizing centers, centrioles, and basal bodies and are implicated in mitosis. Indeed since these assemble into fibers that contract in response to calcium (23–27), understanding the biophysical mechanism of *Vorticella* spasmoneme contraction could be a first step in unraveling the mechanism behind the conformation changes in these systems as well.

SUPPLEMENTARY MATERIAL

To view all of the supplemental files associated with this article, visit www.biophysj.org.

We thank V. Nagarajan and M. Bramucci (DuPont) for useful discussions and H. Buhse (Univ. of Illinois, Chicago) for providing the *Vorticella* strains. A.U. thanks S. Raghavachari and D. Cook for useful discussions.

This work was supported by the DuPont-Massachusetts Institute of Technology Alliance. A.U. was also supported by a Pappalardo Fellowship in Physics.

REFERENCES

1. Katoh, K., and Y. Naitoh. 1992. A mechanosensory mechanism for evoking a cellular contraction in *Vorticella*. *J. Exp. Biol.* 168: 253–267.
2. Amos, W. B. 1975. Contraction and calcium binding in the Vorticellid ciliates. *In* Molecules and Cell Movement. S. Inoue and R. E. Stephens, editors. Raven Press, New York. 411–436.
3. Amos, W. B. 1972. Structure and coiling of the stalk in the peritrich ciliates *Vorticella* and Carchesium. *J. Cell Sci.* 10:95–122.
4. Maciejewski, J. J., E. J. Vacchiano, S. M. McCutcheon, and H. E. Buhse Jr. 1999. Cloning and expression of a cDNA encoding a *Vorticella* convallaria spasmin: an EF-hand calcium-binding protein. *J. Eukaryot. Microbiol.* 46:165–173.
5. Asai, H., T. Ninomiya, R. Kono, and Y. Moriyama. 1998. Spasmin and a putative spasmin binding protein(s) isolated from solubilized spasmonemes. *J. Eukaryot. Microbiol.* 45:33–39.
6. Katoh, K., and M. Kikuyama. 1997. An all-or-nothing rise in cytosolic. *J. Exp. Biol.* 200:35–40.
7. Ochiai, T., H. Asai, and K. Fukui. 1979. Hysteresis of contraction-extension cycle of glycerinated *Vorticella*. *J. Protozool.* 26:420–425.
8. Hoffman-Berling, H. 1958. Der Mechanismus eins neuen, von der Muskelkontraktion verschiedenen Kontraktionszyklus. *Biochim. Biophys. Acta.* 27:247–255.
9. Asai, H., T. Ochiai, K. Fukui, M. Watanabe, and F. Kano. 1978. Improved preparation and cooperative calcium contraction of glycerinated *Vorticella*. *J. Biochem.* (*Tokyo*). 83:795–798.
10. Weis-Fogh, T., and W. B. Amos. 1972. Evidence for a new mechanism of cell motility. *Nature.* 236:301–304.
11. Moriyama, Y., H. Okamoto, and H. Asai. 1999. Rubber-like elasticity and volume changes in the isolated spasmoneme of giant Zoothamnium sp. under Ca^{2+}-induced contraction. *Biophys. J.* 76:993–1000.
12. Katchalski, A., S. Lifson, I. Michaeli, and M. Zwich. 1960. Elementary mechanochemical processes. *In* Contractile Polymers. Pergamon, London. 1–40.
13. Allen, R. D. 1973. Structures linking the myonemes, endoplasmic reticulum, and surface membranes in the contractile ciliate *Vorticella*. *J. Cell Biol.* 56:559–579.
14. Amos, W. B. 1971. Reversible mechanochemical cycle in the contraction of *Vorticella*. *Nature*. 229:127–128.
15. Jones, A. R., T. L. Jahn, and J. R. Fonseca. 1970. Contraction of protoplasm. IV. Cinematographic analysis of the contraction of some peritrichs. *J. Cell. Physiol.* 75:9–19.
16. Moriyama, Y., S. Hiyama, and H. Asai. 1998. High-speed video cinematographic demonstration of stalk and zooid contraction of *Vorticella* convallaria. *Biophys. J.* 74:487–491.
17. Vacchiano, E. J., J. L. Kut, M. L. Wyatt, and H. E. Buhse. 1991. A novel method for mass culturing *Vorticella*. *J. Protozool.* 38: 608–613.
18. Landau, L. D., and E. M. Lifshitz. 1987. Fluid Mechanics. Pergamon Press, Oxford, UK.

19. Keizer, J., G. D. Smith, S. Ponce-Dawson, and J. E. Pearson. 1998. Saltatory propagation of Ca^{2+} waves by Ca^{2+} sparks. *Biophys. J.* 75:595–600.

20. Koch, C. 1999. Biophysics of Computation. Oxford University Press, New York.

21. Shiono, H., and Y. Naitoh. 1997. Cellular contraction precedes membrane depolarization in *Vorticella* convallaria. *J. Exp. Biol.* 200:2249–2261.

22. Mahadevan, L., and P. Matsudaira. 2000. Motility powered by supramolecular springs and ratchets. *Science*. 288:95–100.

23. Hayashi, M., T. Yagi, K. Yoshimura, and R. Kamiya. 1998. Real-time observation of Ca^{2+}-induced basal body reorientation in Chlamydomonas. *Cell Motil. Cytoskeleton.* 41:49–56.

24. Kilmartin, J. V. 2003. Sfi1p has conserved centrin-binding sites and an essential function in budding yeast spindle pole body duplication. *J. Cell Biol.* 162:1211–1221.

25. McFadden, G. I., D. Schulze, B. Surek, J. L. Salisbury, and M. Melkonian. 1987. Basal body reorientation mediated by a Ca^{2+}-modulated contractile protein. *J. Cell Biol.* 105:903–912.

26. Salisbury, J. L. 2004. Centrosomes: Sfi1p and centrin unravel a structural riddle. *Curr. Biol.* 14:R27–R29.

27. Salisbury, J. L., A. Baron, B. Surek, and M. Melkonian. 1984. Striated flagellar roots: isolation and partial characterization of a calcium-modulated contractile organelle. *J. Cell Biol.* 99:962–970.